Research Article

Journal of PeptideScience

Received: 25 January 2011 Revised: 24 March 2011 Accepted: 2 June 2011 Published online in Wiley Online Library: 22 September 2011

(wileyonlinelibrary.com) DOI 10.1002/psc.1391

Apolipoprotein A-I peptide models as probes to formulate potential inhibitors of the low-density lipoprotein oxidation

Maria I. Darvari,[a] Maria P. Petraki,[b] Constantinos Tellis,[b] Konstantinos Harilogis,[b] Alexandros D. Tselepis[b] and Maria Sakarellos-Daitsiotis[b]*

Apolipoprotein A-I (apoA-I), which constitutes the principal protein component of high-density lipoprotein, is responsible for its major antiatherogenic functions. Aiming at contributing to the development of potent inhibitors of low-density lipoprotein (LDL) peptide models of helices 4,6 and 9,10 of apoA-I were designed and synthesized. Specific amino acid substitutions, resulting in transformation of the original helix class A and Y to G according to the Schiffer and Edmundson helical wheel representation, were introduced in order to validate the contribution of these modifications in the inhibitory activity of the synthesized peptide models against the LDL oxidation. The role of Met at positions 112 (helix 4) and 148 (helix 6) as oxidant scavenger was also investigated. The helical characteristics of all the peptide models were studied by CD in membrane-mimicking microenvironments and compared with the original helices. Copyright © 2011 European Peptide Society and John Wiley & Sons, Ltd.

Keywords: apolipoprotein A-I helical peptide models; inhibitors of the LDL oxidation; HDL; CD of apoA-I helices

Introduction

Numerous studies have shown that the high levels of high-density lipoprotein (HDL) and its most abundant protein constituent apolipoprotein A-I (apoA-I) can reduce the risk of atherosclerosis, the leading cause of death in industrialized countries. It is well documented now that apoA-I, which constitutes the principal protein component (70%) of HDL, is responsible for the major functions of HDL as lipid binding and solubilization, cholesterol removal from peripheral cells, activation of lecithin-cholesterol acyltransferase (LCAT) and its antioxidant and anti-inflammatory effects. Several studies have also shown that the intrinsic flexibility of apoA-I allows its structure to acquire different conformations in different lipid environments [1–6].

Based on X-ray crystallography and computer modelling, apoA-I encoded amino acids form 22- and 11-tandem repeats, which are organized in ten amphipathic α-helices, eight α-helical segments of 22 amino acids and two 11-mer repeats that are frequently separated by proline residues.

The N-terminal helix 2 and the C-terminal helix 10 are recognized as important for the initial association with lipids. In the central domain, helix 4 and, to a lesser extent, helix 5 are also very important for lipid binding and the formation of mature HDL, whereas helices 6 and 7 contribute little [4].

A key metabolic role of apoA-I is its ability to activate LCAT, an enzyme which transesterifies the sn-2 fatty acid from phospatidylcholine to cholesterol to yield cholesteryl esters [7]. This role has been devoted to helix 6 of apoA-I, which includes the amino acids sequence 143–164 of apoA-I molecule. Moreover, some of the antioxidant properties of apoA-I have been attributed to specific amino acids in that molecule such as Met at positions 112 of helix 4 and 148 of helix 6 [8]. ApoA-I plays also a central regulatory role in the cholesterol efflux via ABCA1 considering to this action helices 9 and 10 spanning the sequence 209–229 [9–11].

Amphipathic α-helices of apoA-I are assigned to the class A, Y and G depending on the distribution of the positively and negatively charged residues on the polar face [12–17]. The most distinctive feature of the class A helix is the unique clustering of positively charged residues at the polar–non-polar interface and the negatively charged residues at the centre of the polar face. In class Y, positively charged residues are located at the interface and the centre of the polar face, whereas negative-charged residues occupy the rest of the polar face. Class G helices have a random distribution of negative and positive charges around the perimeter of the polar face, in contrast to the highly typical clustering seen in class A [18–25].

Aiming at contributing to the development of potent atheroprotective agents peptide models of helices 4, 6 and 9, 10 were designed and synthesized: specific amino acid substitutions, resulting in transformation of the original helix class A and Y to G according to the Schiffer and Edmundson [26] helical wheel representation, were introduced in order to validate the contribution of these modifications in the antioxidant functions of the peptide models. The role of Met at positions 112 (helix 4)

* *Correspondence to: Maria Sakarellos-Daitsiotis, Department of Chemistry, University of Ioannina, 45110 Ioannina, Greece. E-mail: msakarel@uoi.gr*

a *Department of Medicine, Division of Cardiology, New York University School of Medicine, New York, NY, USA*

b *Department of Chemistry, University of Ioannina, Ioannina, Greece*

Journal of PeptideScience

Table 1. Synthesized peptide models of apoA-I (1–9)

Peptide models	Helix-class	Position in apoA-I	Sequence
1	Helix 4-class Y	104–117	Ac-FQKKWQEEMELYRQ-NH_2
2	Helix 4-class G	104–117 Met^{112} →Ala	Ac-FQKKWQEEAELYRQ-NH_2
3	Helix 6-class A	147–159	Ac-EMRDRARAHVDAL-NH_2
4	Helix 6-class A	147–159 Met^{148} →Ala	Ac-EARDRARAHVDAL-NH_2
5	Helix 6-Class G	147–159 Arg^{149} →Nva Asp^{150} →Orn His^{155} →Ala	Ac-EMNVaOrnRARAAVDAL-NH_2
6	Helix 6-class A	152–164	Ac-ARAHVDALRTHLA-NH_2
7	Helix 6-class G	152–164 Thr^{161} →Lys	Ac-ARAHVDALRKHLA-NH_2
8	Helix 9,10-class Y	209–229	Ac-PALEDLRQGLLPVLESFKVSF-NH_2
9	Helix 9,10-class G	209–229 Asp^{213} →Orn Ser^{224} →Lys	Ac-PALEOrnLRQGLLPVLEKFKVSF-NH_2

and 148 (helix 6) as oxidant scavenger was also investigated. All peptide models (Table 1, 1–9) were tested for their inhibition to the low-density lipoprotein (LDL) oxidation and their conformational characteristics were studied by CD in membrane-mimicking microenvironments.

Materials and Methods

Peptide Synthesis

The synthesis of the peptides was carried out by the stepwise solid-phase procedure SPPS [27,28] on a Rink Amide AM resin (GLBIOCHEM Shang Hai, China) (0.67 mmol/g resin) using the Fmoc methodology. Lys was introduced as Fmoc-Lys-(Boc)-OH (Boc: t-Butoxycarbonyl), glutamic acid as Fmoc-Glu(OtBu)-OH (OtBu: t-Butoxy), glutamine as Fmoc-Gln(Trt)-OH (Trt: Trityl), tryptophan as Fmoc-Trp(Boc)-OH, arginine as Fmoc-Arg(Pbf)-OH (Pbf: 2,2,4,6,7-pentamethyl-dihydrobenzofurane-5-sulfonyl), tyrosine as Fmoc-Tyr(tBu)-OH (tBu: *tert*-butyl), serine as Fmoc-Ser(tBu)-OH, histidine as Fmoc-His(Boc)-OH, Thr as Fmoc-Thr(tBu)-OH, ornithine as Fmoc-Orn(Boc)-OH and aspartic acid as Fmoc-Asp(OtBu)-OH. Fmoc groups were removed using 20% piperidine in DMF. Coupling of each Fmoc-amino acid (3 mol equiv.) was performed in the presence of HBTU/HOBt/DIEA (2.9/3/6 molar ratio). DMF was distilled over ninhydrin to remove traces of amines. Completion of the couplings was ensured by the ninhydrin Kaiser test. Acetylation was performed using a 30 : 1 ratio of acetic anhydride (Ac_2O)/NH_2 groups in pyridine. Peptide models incorporating Met were cleaved from the resin by treatment with TFA/TIS/DMS/H_2O (92.5/2.5/2.5/2.5) and the rest of them with the TFA/TIS/H_2O (95/2.5/2.5) treatment. The resin was removed by filtration, the filtrates were evaporated under reduced pressure and the products were precipitated with cold diethyl ether. Yields range from 80 to 90%. The crude peptides were purified by semi-preparative reverse-phase HPLC on a C_{18} column. Appropriate programmed gradients were applied using eluants A (H_2O/0.1% TFA) and B (CH_3CN/0.1% TFA). The purity of the peptides was checked by analytical HPLC and the correct molecular masses were confirmed by ESI-MS. Molecular weights (M^+) of the peptides are presented in Table 2.

Analytical RP-HPLC

Analytical HPLC of the synthesized compounds (1–9) was performed using a Supelco Discovery (Sigma Aldrich, USA), Waters 616 (USA) (Sigma Aldrich, USA), Waters 616 (USA) C18 (25 cm × 4.6 mm, 5 μm) reverse-phase column with a Waters instrument equipped with a Waters 616 pump and a Waters 2487 (USA) dual λ absorbance detector. Eluent A was 0.1% TFA in water and eluent B was 0.1% TFA in acetonitrile. A linear gradient was used from 10 to 70% acetonitrile in 0.1% TFA at a flow rate of 1 ml/min (1/1/0.05 v/v/v).

Semi-preparative RP-HPLC

RP-HPLC purification was carried out on a SHIMADZU semi-preparative instrument equipped with a SHIMADZU LC-10AD (Shimadzu Corporation, Japan) VP pump and a SHIMADZU SPD-10A VP UV-VIS (Shimadzu Corporation, Japan) VP UV-VIS detector, using a Supelco Discovery C18 (25 cm × 10 mm, 5 μm) column, with the same linear gradient as for analytical RP-HPLC at a flow rate of 4.7 ml/min. Detection was carried out at $\lambda = 214$ nm.

Mass spectroscopy

Positive ion ESI-MS analyses of synthesized compounds 1–9 were performed on a Micromass Platform (Canton, MA 02021 USA) LC-MS. Capillary and cone voltages were set to 3 kV and 35–75 V, respectively. Samples were dissolved in water/acetonitrile/trifluoroacetic acid; molecular weights calculated and found are given in Table 2.

Circular Dichroism

CD spectra were recorded at 25 °C on a Jasco J-815 (Jasco Corporation, Japan) spectropolarimeter equipped with a thermoelectric temperature controller. Spectra were obtained using a quartz cell of 1-mm path length and the concentration of the tested compounds was 10^{-4} M. Experiments were performed in PBS pH 7.4, SDS 8 mM, C_{14}PC 5 mM (dimyristoyl phosphatidylcholine) and TFE/H_20 mixtures (50 : 50 v/v). Spectra were obtained with a 1 nm bandwidth, a scan speed of 50 nm/min and a response of 1 s.

Table 2. Parameters of the synthesis, purification and characterization of peptide models 1–9

Peptide	Yield (%)	RP-HPLC (gradient elution), A : B	t_R (retention time) (min)	ESI-MS
1	85	90 : 10	14	Calculated $[M+H]^+$: 1984.28
		30 : 70		Found $[M+H]^+$: 1985.74
2	79	95 : 5	12.5	Calculated $[M+H]^+$: 1924.15
		30 : 70		Found $[M+H]^+$: 1924.49
3	80	95 : 5	11	Calculated $[M+H]^+$: 1580.78
		30 : 70		Found $[M+H]^+$: 1580.95
4	80	95 : 5	14.5	Calculated $[M+H]^+$: 1520.67
		30 : 70		Found $[M+H]^+$: 1520.90
5	87	90 : 10	19	Calculated $[M+H]^+$: 1456.72
		40 : 60		Found $[M+H]^+$: 1457.32
6	66	90 : 10	21	Calculated $[M+H]^+$: 1471.70
		50 : 50		Found $[M+H]^+$: 1472.05
7	87	90 : 10	11	Calculated $[M+H]^+$: 1498.80
		50 : 50		Found $[M+H]^+$: 1499.63
8	74	70 : 30	12	Calculated $[M+H]^+$: 2399.82
		20 : 80		Found $[M+H]^+$: 2400.72
9	65	90 : 10	16	Calculated $[M+H]^+$: 2439.96
		20 : 80		Found $[M+H]^+$: 2440.72

A, H_2O/0.1% TFA; B, CH_3CN/0.1% TFA.

The signal-to-noise ratio was improved by accumulating three scans. All CD spectra are reported in terms of mean residue molar ellipticity (θ) in degree cm^2/dmol). The percentage helical content was estimated on the basis of the $[\Theta]_{222}$ nm values, in different environments, as described by Chen *et al*. [29].

LDL Isolation and Oxidation

LDL (d = 1.019–1.063 g/ml) was isolated from freshly prepared human plasma supplemented with 0.01% EDTA (w/v) and 5 mg/ml gentamicin sulfate Garamycin, Schering-Plough, (NY, USA) by sequential centrifugation in a Beckman L7-65 ultracentrifuge at 40 000 rpm, 14 °C with a Type NVT 65 rotor [30]. LDL was filter sterilized (0.22 mM, Millipore, Billerica, MA, USA) and stored in the dark at 4 °C under nitrogen for up to 2 weeks. LDL protein was determined by the bicinchoninic acid method. Purity of the LDL preparation was assessed by agarose gel electrophoresis Hydragel Lipo ad Lp(a) Kit (Sebia, Norcross, GA 30093, USA). Before oxidation, LDL was extensively dialysed (to remove EDTA) against two changes of a 200-fold volume of 10 mM PBS for 24 h at 4 °C in the dark. LDL (100 µg protein/ml) was incubated in the presence of copper sulfate (5 µM final concentration) [31]. In selected experiments LDL (100 µg protein/ml) was oxidized with met-myoglobin/H_2O_2 (10 and 50 mM, respectively) in the presence of diethylenetriaminepentaacetic acid (DTPA) (0.1 mM) [17].

In all oxidation studies, peptides were dissolved in PBS, pH 7.4, and used at final concentration ranging from 40 to 424 µM. The kinetics of oxidation were determined by monitoring the increase in absorbance at 234 nm every 10 min for 6 h. The lag time of peptide oxidation was calculated as previously described [32].

Results and Discussion

One of the mechanisms by which HDL might be antiatherogenic is by protecting LDL from oxidation and inhibiting the proatherogenic effect of oxLDL *in vitro* and *in vivo*. ApoA-I, one of the main constituents of HDL, which plays a critical role to the HDL functions, remains a challenging goal for the development of potent atheroprotective agents.

Association of apoA-I with lipids, a crucial functional step of apoA-I, do not appear to be simply related to the hydrophobicity of the protein α helices but also to the distribution of charged residues along the helix, which is directly implicated to the different classes of α helices. Peptide models obtained by the conversion of the most abundant classes A and Y to class G were designed, synthesized and studied in order to investigate the effect of the random distribution of the positive and negative charges on the polar phase of the helices in their conformational and biological properties.

Substitution of $Arg^{149} \rightarrow$Nva, $Asp^{150} \rightarrow$Orn and $His^{155} \rightarrow$Ala in peptide model 3, helix 6 class A, resulted in the formation of a class G peptide model (5). Substitution of Thr^{161} for Lys in helix 6 (peptide model 6) converted also class A to class G peptide model (7). Replacement of $Asp^{213} \rightarrow$Orn and $Ser^{224} \rightarrow$Lys in helix 9,10 class Y (peptide model 8) created a class G peptide model (9) (Table 1).

Among the four Met residues comprised within the amino acid sequence of apoA-I, two of them at positions 112 and 148 are likely to play an important role as oxidant scavengers [33]. Met^{112} and Met^{148} in helix 4 and 6 respectively were substituted by Ala and the antioxidant effects of the resulting peptide models (2,4) were compared with the initial helices (1,3) (Table1).

Helices 4,6 and 9,10, as well as their substituted models were synthesized according to the solid-phase peptide method in good yields and high purity. Parameters of the synthesis, purification and characterization of peptide models 1–9 are given in Table 2.

The CD spectra of peptide models 1–9 in SDS, at the critical micelle concentration 8 mM, and in C_{14}PC 5 mM exhibited a positive band at 192 nm and two negative bands at 205 and 222 nm typical of helical structure (Figures1 and 2). Their helical content, estimated on the basis of the $[\Theta]_{222}$ value, ranged from 32 (6,8) to 83% (5) in SDS and from 29 (3,4) to 62% (5) in

Journal of PeptideScience

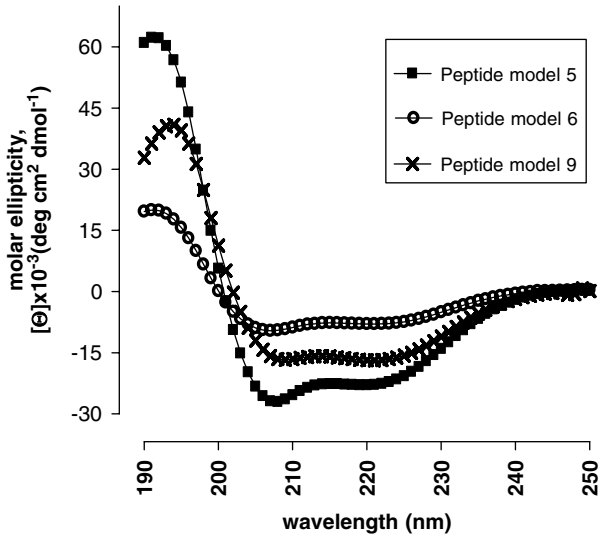

Figure 1. CD spectra of peptide models 5, 6 and 9 in SDS 8 mM.

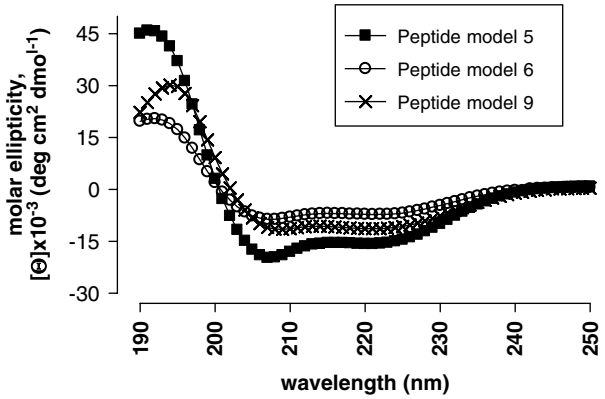

Figure 2. CD spectra of peptide models 5, 6 and 9 in C_{14}PC 5 mM.

C_{14}PC, whereas in phosphate-buffered saline (PBS) they adopt random structure. These findings point out that the synthesized models experience helical conformations in membrane-mimicking microenvironments. The helical conformation of all peptide models was also preserved in TFA/H_2O mixtures (50 : 50 v/v), ranged from 22 to 70%, as TFA is a solvent that favours the helix.

It deserves to be mentioned that transformation of class A helix 6 (147–159) (3) to class G (5) duplicated the helical content in C_{14}PC (from 30 to 60%) and enhanced the helix from 50 to 83% in SDS. Significant increase of the helical features of class A helix 6 (152–164) (6) and class Y helix 9,10 (209–229) (8) was also observed after their alterations to class G (7,9). One may assume that transformation of class A and Y to G increased the helical characteristics of the helices, which is attributed to a more favourable distribution of the charges on the polar phase of G compared to A and Y.

The inhibitory activity of the synthesized peptide models (1–9) was evaluated on the basis of their ability to increase the resistance of isolated LDL to copper-induced oxidation *in vitro*. The kinetics of the oxidation were determined by monitoring the increase of the absorbance at 234 nm in various peptide concentrations. All the tested peptides (1–9) increased the lag time of LDL oxidation

Table 3. Effect of the apoA-I peptide models 1–9 on Cu^{2+}-induced LDL oxidation

Peptide model	Concentration (μM)	Lag time (min)	Reduction of the oxidation rate (%)	Reduction of total dienes (%)
–	0	60 ± 10	–	–
1	424	86	67	50
2	424	70	40	22
3	318	160	65	8.7
4	318	100	10	8
5	40	–	100	100
6	53	–	100	100
7	424	110	45	2
8	424	90	27	5.4
9	424	120	40	8

and decreased the maximal rate of conjugated diene formation (rate of oxidation), as well as the total amount of dienes formed during oxidation, in a dose-dependent manner (Table 3).

Peptide model 3 corresponding to helix 6 (147–159) class A increased the lag time of LDL oxidation (from 60 to 160 min) and decreased the rate of oxidation to 64% and the diene formation to 8.7% in a dose-dependent manner (range of concentrations 53–318 μM) (Figure 3(A), Table 3). Peptide model 5, obtained from the conversion of class A to class G, exhibited a significantly more potent inhibitory effect compared to 3 as its threshold concentration was 40 μM *versus* 318 μM of 3 (Table 3). In fact the random distribution of positive and negative charges on the polar face of class G, in contrast to the typical clustering of class A, as well as the relatively high percentage of helical conformation, defined by CD, seems to favour the inhibition of the peptide model 5 on the LDL oxidation (Figure 3(B)).

The inhibitory effect of peptide models on Cu^{2+}-induced LDL oxidation was rather potent as the peptide model 6 corresponding to helix 6 (152–164) class A (6) inhibited oxidation completely at the concentration 0.53 μM. On the contrary the inhibitory properties of model 7 class G, resulting from model 6 after the substitution of Thr^{161} for Lys, were relatively weak. The rate of oxidation decreased to 45% and the diene formation to 2% (range of concentrations 0.53–424 μM). It is likely that replacement of Thr from Lys modified the hydrophobicity of model 7 and diminished its activity (Table 3).

Peptide model 8 spanning the sequence 209–219 of helices 9,10 class Y reduced the rate of oxidation to 27% and the diene formation to 5.4% (concentrations from 53 to 424 μM). Peptide model 9 class G obtained by substitution of Asp^{213} →Orn and Ser^{224} →Lys showed 40% depletion of the LDL oxidation rate and 8% reduction of the diene formation (concentrations ranged from 53 to 424 μM). These findings point out that the transformation of peptide model 8 from class Y to class G, as well as the enhancement of helix, stimulates the inhibitory activity of the resulting peptide model 9 (Figure 4 and Table 3).

Oxidation of LDL in the presence of peptide model 1, which incorporates Met at position 112, was inhibited considerably as the decrease of the oxidation rate and the diene formation reached 67 and 50%, respectively (concentrations from 53 to 424 μM). On the contrary, substitution of Met^{112} by Ala (2) reduced the rate of oxidation and the diene formation to 40 and 22% respectively confirming the role of Met as an oxidant scavenger. Peptide models 3 and 4 showed comparable activities (~65% reduction

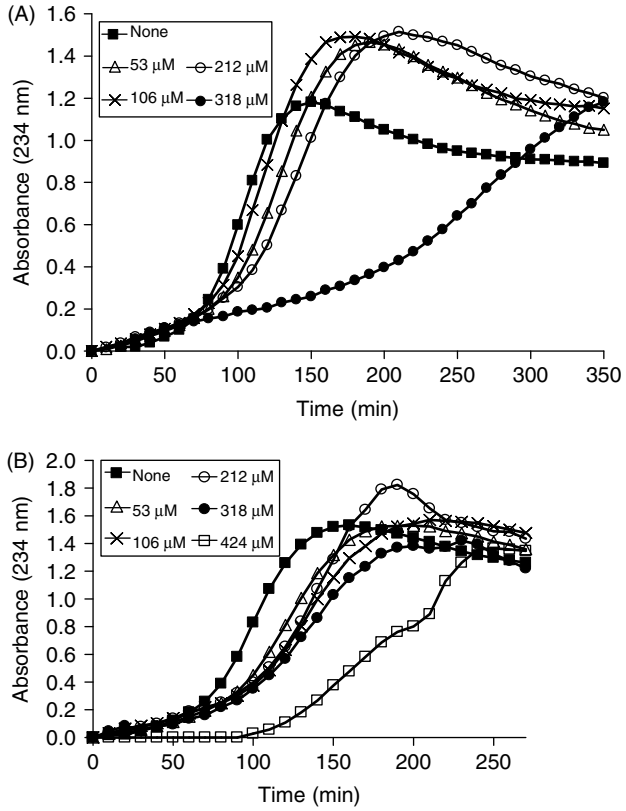

Figure 3. Sigmoid oxidation curves illustrating the dose-dependent inhibition of LDL oxidation induced by the peptide model 3 (A) and 9 (B).

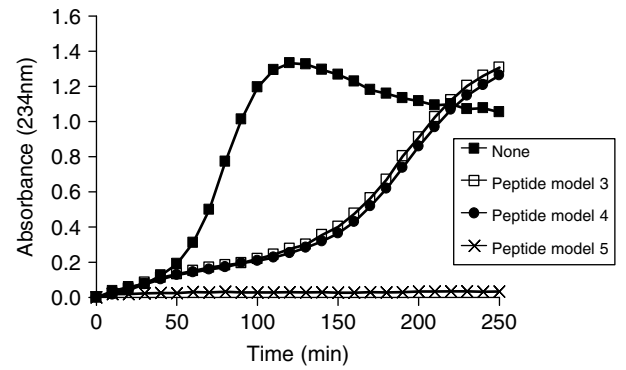

Figure 4. Sigmoid oxidation curves illustrating the dose-dependent inhibition of LDL oxidation induced by the peptide models 3, 4 and 5 at 424 μMU.

of the oxidation rate and ~8% reduction of the diene formation) indicating that the replacement of Met^{148} (3) by Ala (4) was not crucial (Table 3).

According to our previously published results, purified apoA-I, almost completely inhibits Cu^{2+}-induced LDL oxidation at a concentration of 321 μM [17]. In the present study, the peptide models 5 and 6 completely inhibit LDL oxidation at a concentration of 40 and 53 μM, respectively, thus these peptides are sixfold to eightfold more potent compared with apoA-I. To test the possibility of these peptides acting as transition metal chelators, through their polar side chains, we studied their effect on LDL oxidation performed in the presence of met-myoglobin/H_2O_2 and DTPA a

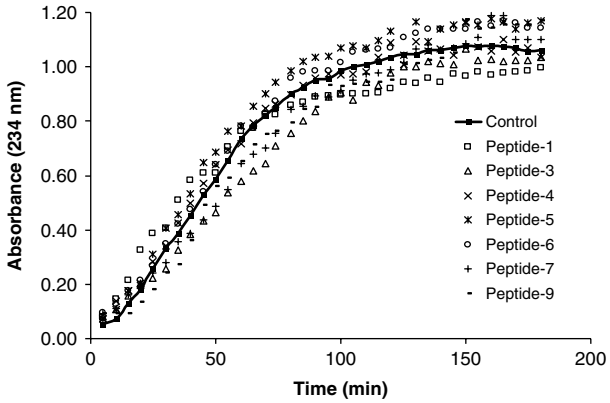

Figure 5. Representative curves of LDL oxidation with met-myoglobin/H_2O_2/DTPA in the presence of peptide models at 424 μM.

system that lacks free iron ions as any possible contaminating iron is chelated with DTPA [17]. The interaction of met-myoglobin with H_2O_2 leads to the formation of ferryl myoglobin-free radicals that are able to oxidize vulnerable targets, like unsaturated lipids [34]. The amount of total dienes formed during LDL oxidation reached a maximum of 215±54 nmol/mg protein at 80±10 min of oxidation. Similar oxidation curves were obtained in the presence of all peptides tested (Figure 5), indicating that peptide models failed to inhibit LDL oxidation performed in the absence of transition metals. These results suggest that the antioxidant effect of peptide models investigated in this study is at least partially attributed to transition metal chelation. However, the enhanced antioxidant activity of peptide models 5 and 6, from tenfold to eightfold compared with the rest, indicates their effectiveness in protecting LDL from oxidation.

Conclusions

Our study points out that the conversion of the apoA-I helices from one class to another might affect their biological properties as the charge distribution on the polar phase of the helices is related to their affinities towards lipoproteins. Thus, alteration of class A and Y peptide models (3 and 8) to class G (5 and 9) augmented their antioxidant activities. In particular peptide model 5, derived from the conversion of model 3 (class A) to G, inhibited the LDL oxidation at a relatively low concentration 40 μM. However, substitution of Thr for Lys in peptide model 6 (class A) abolished the activity of model 7 (class G) indicating how perceptive is the balance of the charges on the polar phase of the helix. The contribution of Met at positions 112 and 148, as oxidant scavengers, was also confirmed as their replacement reduced the antioxidant properties of models 2 and 4. It is concluded that modifications of the apoA-I helices might lead to the formulation of potential atheroprotective peptide model candidates.

References

1 Fielding CJ, Fielding PE. Molecular physiology of reverse cholesterol transport. *J. Lipid Res.* 1995; **36**: 211–228.
2 Natarajan P, Forte TM, Chu B, Phillips MC, Oram JF, Bielicki JK. Identification of an apolipoprotein A-I structural element that mediates cellular cholesterol efflux and stabilizes ATP binding cassette transporter A1. *J. Biol. Chem.* 2004; **279**: 24044–24052.

3 Brouillette CG, Anantharamaiah GM. Structural models of human apolipoprotein A-I. *Biochim. Biophys. Acta* 1995; **1256**: 103–129.
4 Frank PG, Marcel YL. Apolipoprotein A-I: structure-function relationships. *J. Lipid Res.* 2000; **41**: 853–872.
5 Brewer HB, Jr. Fairwell T, LaRue A, Ronan R, Houser A, Bronzert TJ. The amino acid sequence of human APOA-I, an apolipoprotein isolated from high density lipoproteins. *Biochem. Biophys. Res. Commun.* 1978; **80**: 623–630.
6 Zannis VI, Cole FS, Jackson CL, Kurnit DM, Karathanasis SK. Distribution of apolipoprotein A-I, C-II, C-III, and E mRNA in fetal human tissues. Time-dependent induction of apolipoprotein E mRNA by cultures of human monocyte-macrophages. *Biochemistry* 1985; **24**: 4450–4455.
7 Fielding CJ, Shore VG, Fielding PE. Lecithin: cholesterol acyltransferase: effects of substrate composition upon enzyme activity. *Biochim. Biophys. Acta* 1972; **270**: 513–518.
8 Roberts LM, Ray MJ, Shih TW, Hayden E, Reader MM, Brouillette CG. Structural analysis of apolipoprotein A-I: limited proteolysis of methionine-reduced and -oxidized lipid-free and lipid-bound human apo A-I. *Biochemistry* 1997; **36**: 7615–7624.
9 Acton S, Rigotti A, Landschulz KT, Xu S, Hobbs HH, Krieger M. Identification of scavenger receptor SR-BI as a high density lipoprotein receptor. *Science* 1996; **271**: 518–520.
10 Zhao Y, Sparks DL, Marcel YL. Specific phospholipid association with apolipoprotein A-I stimulates cholesterol efflux from human fibroblasts. Studies with reconstituted sonicated lipoproteins. *J. Biol. Chem.* 1996; **271**: 25145–25151.
11 Castro GR, Fielding CJ. Early incorporation of cell-derived cholesterol into pre-beta-migrating high-density lipoprotein. *Biochemistry* 1988; **27**: 25–29.
12 Li WH, Tanimura M, Luo CC, Datta S, Chan L. The apolipoprotein multigene family: biosynthesis, structure, structure-function relationships, and evolution. *J. Lipid Res.* 1988; **29**: 245–271.
13 Nolte RT, Atkinson D. Conformational analysis of apolipoprotein A-I and E-3 based on primary sequence and circular dichroism. *Biophys. J.* 1992; **63**: 1221–1239.
14 Borhani DW, Engler JA, Brouillette CG. Human apolipoprotein A-I: structure determination and analysis of unusual diffraction characteristics. *Acta Crystallogr. D Biol. Crystallogr.* 1999; **55**: 2013–2021.
15 Borhani DW, Rogers DP, Engler JA, Brouillette CG. Crystal structure of truncated human apolipoprotein A-I suggests a lipid-bound conformation. *Proc. Natl. Acad. Sci. U.S.A.* 1997; **94**: 12291–12296.
16 Segrest JP, Jones MK, De Loof H, Brouillette CG, Venkatachalapathi YV, Anantharamaiah GM. The amphipathic helix in the exchangeable apolipoproteins: a review of secondary structure and function. *J. Lipid Res.* 1992; **33**: 141–166.
17 Beaufils C, Alexopoulos C, Petraki MP, Tselepis AD, Coudevylle N, Sakarellos-Daitsiotis M, Sakarellos C, Cung MT. Conformational study of new amphipathic alpha-helical peptide models of apoA-I as potential atheroprotective agents. *Biopolymers* 2007; **88**: 362–372.
18 Segrest JP, De Loof H, Dohlman JG, Brouillette CG, Anantharamaiah GM. Amphipathic helix motif: classes and properties. *Proteins* 1990; **8**: 103–117.
19 Ajees AA, Anantharamaiah GM, Mishra VK, Hussain MM, Murthy HM. Crystal structure of human apolipoprotein A-I: insights into its protective effect against cardiovascular diseases. *Proc. Natl. Acad. Sci. U.S.A.* 2006; **103**: 2126–2131.
20 Gorshkova IN, Liadaki K, Gursky O, Atkinson D, Zannis VI. Probing the lipid-free structure and stability of apolipoprotein A-I by mutation. *Biochemistry* 2000; **39**: 15910–15919.
21 McLachlan AD. Repeated helical pattern in apolipoprotein-A-I. *Nature* 1977; **267**: 465–466.
22 Oda MN, Forte TM, Ryan RO, Voss JC. The C-terminal domain of apolipoprotein A-I contains a lipid-sensitive conformational trigger. *Nat. Struct. Biol.* 2003; **10**: 455–460.
23 Okon M, Frank PG, Marcel YL, Cushley RJ. Heteronuclear NMR studies of human serum apolipoprotein A-I. Part I. Secondary structure in lipid-mimetic solution. *FEBS Lett.* 2002; **517**: 139–143.
24 Rogers DP, Brouillette CG, Engler JA, Tendian SW, Roberts L, Mishra VK, Borhani DW. Truncation of the amino terminus of human apolipoprotein A-I substantially alters only the lipid-free conformation. *Biochemistry* 1997; **36**: 288–300.
25 Zhu HL, Atkinson D. Conformation and lipid binding of the N-terminal (1–44) domain of human apolipoprotein A-I. *Biochemistry* 2004; **43**: 13156–13164.
26 Schiffer M, Edmundson AB. Use of helical wheels to represent the structures of proteins and to identify segments with helical potential. *Biophys.J.* 1967; **7**: 121–135.
27 Bodansky M, Bodansky A. Activation and coupling. In *The practice of Peptide Synthesis*. 2nd edn, Bodansky M, Bodansky A (eds). Springer-Verlag: Berlin, Heidelberg, 1994; 75–125.
28 Giralt E, Albericio F. Synthesis of peptide on solid supports. In *Synthesis of Peptide and Peptidomimetics*. Vol. E22a: Synthesis of peptides, (Goodman M, Felix A, Moroder L, Toniolo G (eds). Georg Thieme Verlag: Stuttgard, New York, 2003; 665–824.
29 Chen YH, Yang JT, Martinez HM. Determination of the secondary structures of proteins by circular dichroism and optical rotatory dispersion. *Biochemistry* 1972; **11**: 4120–4131.
30 Liapikos TA, Antonopoulou S, Karabina SP, Tsoukatos DC, Demopoulos CA, Tselepis AD. Platelet-activating factor formation during oxidative modification of low-density lipoprotein when PAF-acetylhydrolase has been inactivated. *Biochim. Biophys. Acta* 1994; **1212**: 353–360.
31 Tselepis A, Doulias P, Lourida E, Glatzounis G, Tsimoyiannis E, Galaris D. Trimetazidine protects low-density lipoproteins from oxidation and cultured cells exposed to H(2)O(2) from DNA damage. *Free Radic. Biol. Med.* 2001; **30**: 1357–1364.
32 Karabina SA, Liapikos TA, Grekas G, Goudevenos J, Tselepis AD. Distribution of PAF-acetylhydrolase activity in human plasma low-density lipoprotein subfractions. *Biochim. Biophys. Acta* 1994; **1213**: 34–38.
33 Garnet B, Waldeck AR, Witting PK, Rye KA, Stocker R. Oxidation of high density lipoproteins–II. Evidence for direcret reduction of lipid hydroperoxides by methionine residues of apolipoproteinsAI and AII. *J. Biol. Chem.* 1998; **273**: 6088–6095.
34 Galaris D, Korantzopoulos P. On the molecular mechanism of metmyoglobin-catalyzed reduction of hydrogen peroxide by ascorbate. *Free Radic. Biol. Med.* 1997; **22**: 657–667.

